Doi.org/10.36721/PJPS.2024.37.6.REG.1505-1515.1

Neuroprotective effect of sinapic acid in APP/PS1 mouse model and PC12 Cells of Alzheimer's disease via activation of PI3K/Akt/GSK3β signaling pathways

Di Xue, Yuchao Liu, Tao Xu, Fangyi Pei and Li Fan*
Qiqihar Medical University, Qiqihar, China

Abstract: To explore the neuroprotective effects of Sinapic Acid (SA) in APP/PS1 mouse model and amyloid beta-peptide (Aβ)-induced neuronal cell apoptosis using PC12 cells of Alzheimer's disease. *In vivo*, the Morris water maze (MWM) test assessed learning and memory abilities, enzyme-linked immunosorbent assay test and immunohistochemistry were conducted to plaque deposition and content of Aβ. Western blotting was performed to p-P13K, P13K, p-Akt, Akt, p-GSK3β and GSK3β expression of the hippocampus in mice, respectively. *In vitro*, the viability of the cells, the apoptosis of the cells and the level of Bax, Bcl-2, caspase-3, p-P13K, P13K, p-Akt, Akt, p-GSK3β, and GSK3β expression of PC12 cells were examined by CCK-8 assay, Hoechst 33342 and Calcein/propidium iodide (PI) staining, flow cytometry and Western blotting, respectively. Our results indicated SA could improve learning and memory abilities and decrease plaque deposition and content of Aβ of the hippocampus in mice. Furthermore, SA increased cell viability and lessened cell apoptosis by increasing the ratio of Bcl-2/Bax, lessening protein levels of Caspase-3 in PC12 cells. SA upregulated the phosphorylation expression level of PI3K/Akt/GSK3β in APP/PS1 mice and PC12 cells. Our research showed that SA's neuroprotective effect reduced Aβ deposition and cell apoptosis by activating the PI3K/Akt/GSK3β pathway.

Keywords: Sinapic acid, β-amyloid protein, cell apoptosis, PI3K/Akt/GSK3β signaling pathway.

Submitted on 30-04-2024 – Revised on 16-10-2024 – Accepted on 22-10-2024

INTRODUCTION

Alzheimer's disease (AD) is a cognitive impairment disorder that primarily affects the elderly. (Rajendran *et al*, 2024). The manifestation of AD manifests in the accumulation of β-amyloid protein (Aβ) aggregations, resulting in the formation of age spots (APs) and neurofibrillary tangles (NFTs). These developments are triggered by the tau protein's hyperphosphorylation, neurite alterations, and the loss of nerve cells (Breijyeh *et al*., 2020). Aβ is a peptide fragment from β-secretory and γ-secretory enzyme cleaving of amyloid precursor protein processing (APP) (Caruso *et al*., 2019). Releasing Aβ into the rat brain induces memory impairment and neuronal damage. At the same time, abnormal Aβ deposition and a large amount of nerve cell damage are typical in the AD population, suggesting that Aβ-induced nerve cell damage may be an important cause of AD (Liu *et al*., 2022). In addition, considerable evidence has indicated that $Aβ_{1-42}$, the main component of Aβ, which is more neurotoxic, can cause degeneration of the nervous system, produce neurotoxic effects on nerve cells, and lead to nerve cell damage (Li *et al*., 2024). Therefore, eliminating excessive accumulation of Aβ and inhibiting Aβ-induced neuronal degeneration may be an effective method to prevent AD development.

The PI3K/Akt signaling pathway is one of the pathways that regulate nerve cell survival, differentiation and apoptosis (Kumar *et al*., 2022). LY294002 is a specific inhibitor of PI3K, which can specifically inhibit the PI3K/Akt signaling pathway, such as inhibiting Akt phosphorylation (Zhang *et al*., 2020). In addition, Glycogen synthase kinase 3β (GSK3β) is negatively regulated by Akt as an essential substrate of Akt, which is closely related to tau protein hyperphosphorylation, leading to nerve cell apoptosis. Relevant research finds that tau protein hyperphosphorylation may be caused by abnormal production and deposition of Aβ (Matsuda *et al*., 2019). It has been considered that the Neurotoxicity of Aβ is related to the PI3K/Akt/GSK3β signaling pathway (Wang *et al*., 2023).Therefore, finding targeted drugs that regulate the PI3K/AktGsk3β signaling pathway and resist the neurotoxicity of Aβ may be one of the effective measures to prevent and treat AD.

Sinapic Acid (SA) is a natural cinnamic acid widely found in the plant kingdom, such as rice, oats, buckwheat, etc. In addition, It is found in high levels in fermented foods such as wine and vinegar. It has anti-oxidation, anti-inflammation, anti-cancer and other pharmacological effects (Ikeda *et al.,* 2021). Due to its strong lipophilic properties, SA can traverse the blood-brain barrier, allowing it to enter the central nervous system and improve memory function in mice. Previous studies have attested that SA could effectively protect neuro cells (Pandi *et al.,* 2021). However, the protective mechanism of SA against neural damage induced by $Aβ_{1-42}$ is still unknown.

**Corresponding author:* e-mail: fan123456li@126.com

This study delved into the neuroprotective impact of SA on AD through the PI3K/Akt/GSK3β signaling pathway, potentially opening up novel avenues for clinical AD treatment.

MATERIALS AND METHODS

Chemicals

SA (purity > 98% (HPLC), B25310, Shanghai yuanye Bio-Technology, China); $A\beta_{1-42}$ (purity ≥95% (HPLC), A9810, Sigma, Germany); Dimethyl sulfoxide (DMSO) (D8418, Sigma, Germany); LY294002 (M1925, AbMole, USA); Mouse Amyloid β Protein 42 ELISA kit (JL11386, Jonln Biotechnology, China); Immunohistochemistry detection system kit (IHC001, Bioss Biotechnology, China); Cell Counting Kit-8 (CCK-8) assay kit(C0037), Hoechst 33342 (C1025), Calcein/PI Calcein/PI Cell Activity and Cytotoxicity Detection Kit (C2015) and Assay Kit Annexin V-FITC apoptosis detection kit(C1062) purchased from Beyotime Biotechnology (China); Anti-$A\beta_{1-42}$ (ab201061), Anti-rabbit IgG (Alexa Fluor 488, ab150077), Anti-Bcl-2(ab32124), Bax (ab182733) and caspase-3(ab179517) purchased from Abcam (USA); PI3K(4292), Akt (9272), Anti-phospho-PI3K (4228), and phospho-Akt (4060), β-actin purchased from CST(USA); ECL western blotting detection reagents (A38555, Thermo Fisher Scientific, USA).

Animals and treatment

APPswe/PSEN1dE9 (APP/PS1) and C57BL/6 male mice of 8 months weighted 30g were kindly provided by Shanghai Sippe-Bk Lab Animal Co., Ltd. (Permit Number: SCXK (Hu) 2018-0006). Mice were kept in groups of five in cages in a sterile breeding environment with noise below 80 decibels, 12 hours of lighting/12 hours of alternating darkness, temperature (20-25)□, humidity (60±10)%, sufficient water, and food. The mice were changed the padding twice a week and complied with the requirements of the Animal Ethical Care Committee (QMU-AECC-2021-232). Following a 7-day acclimatization period, the APP/PS1 mice underwent random allocation into various groups, specifically the APP/PS1 group, 5mg/kg SA group labeled APP/PS1 + SA-L, 7.5mg/kg SA group designated as APP/PS1 + SA-M, 10mg/kg SA group denoted APP/PS1 + SA-H. Additionally, the C57BL/6 mice group served as the control. The mice were then administered SA orally at 5, 7.5 and 10mg/kg dosages for one week.

Cell culture and drug preparation

Rat pheochromocytoma (PC12) cells were obtained from the Institute of Biochemistry and Cell Biology (Shanghai, China), were cultivated in RPMI 1640 medium under conditions of 37°C and 5% CO_2 atmosphere. Passage number for PC12 cell lines is 2 to 3 for experimentation. $A\beta_{1-42}$ solution (1mM) with DMSO was incubated at 37°C for 7 days to facilitate aggregation. Subsequently, it was diluted to the desired concentrations for further experimentation. Similarly, DMSO serves as a solvent to dissolve SA (50mM).

Morris water maze (MWM) test

The MWM mainly consists of a water tank and a movable platform. The mice had received training four times a day for five days. After completing all the training, the MWM was dismantled, and the mice were randomly placed into the water. Subsequently, the time taken by the mice to reach the previous platform location and their swimming paths within 60 seconds were documented. Assays were repeated at least three times.

Immunohistochemistry

Immunohistochemistry procedures were executed on hippocampus tissue samples. Initially, the samples underwent dewaxing and hydration steps. Subsequently, the rabbit anti-$A\beta_{1-42}$ primary antibody was incubated overnight at 4ºC with a dilution ratio of 1:600. Then incubate, primary and secondary antibodies, labeled with Alexa Fluor 488, diluted at a ratio of 1:800, for 15 minutes. Then, the washing process was completed three times with PBS (0.02M, PH=7.4, without calcium and magnesium) and a dripped addition of horseradish enzyme labeled streptomycin ovalbumin working solution for 20 minutes. After washing, 50μL of DAB was used to develop color, restained with hematoxylin for 5 sec, rinsed for 5 minutes, gradient alcohol drying, transparent with xylene and sealed. Ultimately, the hippocampus tissues were observed using a fluorescent microscope (LSM 710, Zeiss, Germany). Zeiss Axio Observer LSM710 inverted microscope with manual XY stage (250x230mm travel) of universal mounting frame K. Z-focus drive with 13mm range and 25nm step size. Equipped with 5x/0.16 WD, 10x/0.30 WD, 20x/0.4 Corr WD, 40x/0.6 Corr WD, 100x/1.3 Oil WD. DAPI/FITC/Texas Red filter cubes. X-Cite 120LED light source. 6144x6144 pixels, 0.02μm pixel size, 16 Bit. IOD was obtained as the accumulation of the optical density values of each point on the image. The area was the area of the antigen with positive reactions in the field of view. The average optical density value AOD=IOD/Area.

Enzyme-linked immunosorbent assay (ELISA)

Levels of $A\beta_{1-42}$ were determined by Mouse Amyloid β Protein 42 ELISA kit. Hippocampus tissue of the mice in each group with the same weight were collected and placed it in PBS. Hippocampus tissues were lysed with ultrasonic method, then centrifuged them at 5,000 r/min for 15 min and took the supernatant. Finally, the concentrations of $A\beta_{1-42}$ were ascertained in accordance with the guidelines provided by the ELISA kit. PBS was osmotic pressure control group. Subsequently, the absorbance was determined at 450nm. Assays were repeated at least three times.

Cell Viability Assay

PC12 cells were planted in 96-well plates for 24h (1×10^4 /well). LY294002 (10μM), an inhibitor of the

PI3K/Akt/GSK3β signaling pathway, was added 1 hour before $A\beta_{1-42}$ and (or) SA. After treatment with $A\beta_{1-42}$ (0–16μM) or SA (0-200μM) or coprocessing for 24h, incubate with CCK8 for 2h. Then, cell viability was performed using the same method as the ELISA protocol. Assays were repeated at least three times.

Hoechst 33342 and Calcein/PI Staining

PC12 cells were planted in 6-well plates for 24 h (1×10^5 /well), followed by SA (25, 50 and 100μM) exposed to $A\beta_{1-42}$ (2μM) for 1d. Afterward, PC12 cells were stained in darkness with Hoechst 33342 or Calcein/PI solution for 0.5 h. Finally, PC12 cells were photographed under a fluorescent microscope (LSM 710, Zeiss, Germany).

Flow Cytometry Analysis of Apoptosis

Perform the test according to the instructions of the apoptosis assay kit.

Western Blot Analysis

Extract total proteins from hippocampal tissue and PC12 cells and measure their concentrations using the BCA assay kit. Block an equal amount of deformable protein on a polyvinylidene fluoride (PVDF) membrane with a 5% blocking solution at RT for 1 hour. Incubate overnight at 4°C with primary antibodies against Bax (1:1000), Bcl-2 (1:1000), Caspase-3 (1:500), P13K (1:1000), p-P13K (1:800), Akt (1:1000), p-Akt (1:800), and β- actin (1:1000). Then, the secondary antibody was incubated for 2 hours (RT). Subsequently, the membrane bands were detected using an ECL kit under a Chemiluminescent Imaging System (Bio-Rad, USA).

STATISTICAL ANALYSIS

All data are presented as mean ± standard error of the mean. One way analysis of variance and unpaired Student's t-test were used to analyze differences between groups. Statistical significance was set at $P < 0.05$. Statistical analyses were performed using GraphPad Prism 6.0 (GraphPad Software, San Diego, CA, USA).

RESULTS

Effect of SA on Cognitive Function in Mice

As shown in fig. 1A, we conducted experiments using the Morris Water Maze (MWM) and found that the escape latency of APP/PS1 mice was significantly prolonged. Moreover, escape latency had no significant difference in escape latency after being treated with SA on day 1. The escape latency in WT and SA-treated APP/PS1 mice was reduced during the next 4 days.

After SA processing had been completed, the number of intersections in the platform area had increased (vs. Model, $p<0.01$ or $p<0.05$)(fig. 1B). Equally, APP/PS1 mice spent less distance and time than the control group ($p<0.01$). The percentage of distance and time spent in the target zone was increased significantly in the mice by administration of SA compared to the WT mice (fig. 1C, D). The movement trajectories of each group for space exploration in the hidden platform trail are shown in fig. 1E. These results demonstrate SA treatment ameliorated memory deficiency and spatial learning in APP/PS1 mice.

Effect of SA on the Plaque of Aβ in Hippocampus Tissue in Mice

The IHC method was used to evaluate the deposition of Aβ plaques in the hippocampal area of mice. The Aβ positive plaque appears brown (fig. 2A). The Aβ plaque in WT mice's hippocampal area was relatively small, and the sedimentation color is light brown. Compared to WT mice, APP/PS1 mice had more plaque of Aβ in the hippocampus area, and the area occupied by sedimentation increased and the color deepened. After intervention with SA, the sedimentation area decreases, and the plaque color becomes lighter. Furthermore, the quantitative analysis was used to study the AOD values of the mice (fig. 2B). The AOD values of APP/PS1 mice were increased in contrast with WT mice($p < 0.01$). AOD values of SA-treated mice were decreased ($p < 0.01$ or $p < 0.05$). Results displayed SA reduced plaque deposition of Aβ in hippocampus tissue in mice.

Effect of SA on Content of $A\beta_{1-42}$ in Hippocampus Tissue in Mice

As shown in fig. 2C, compared with WT mice, the content of $A\beta_{1-42}$ in APP/PS1 mice were higher ($p < 0.01$), while SA decreased its content ($p < 0.01$ or $p < 0.05$). It had been proven that SA could inhibit the abnormal increase in $A\beta_{1-42}$.

Effects of SA on the Protein Expression of P13K/Akt/GSK3β in Hippocampus Tissue in Mice

As shown in fig. 3(A-D), there was no significant difference in the expression of P13K, Akt, and GSK3β among each group. Still, compared with WT mice, the ratios of p-P13K/t-P13K, p-Akt/t-Akt and GSK3β/p-GSK3β in the hippocampus tissue of APP/PS1 mice were reduced remarkably ($p<0.01$ or $p<0.01$). After SA treatment, the p-P13K/t-P13K and p-Akt/t-Akt ratios were higher than the model group ($p<0.05$ or $p<0.01$). In summary, SA activated P13K/Akt/GSK3β pathway by promoting P13K, Akt, GSK3β phosphorylation.

Effects of SA on Aβ1–42-Induced Cytotoxicity in PC12 Cell Injury

We first tested the cytotoxicity of $A\beta_{1-42}$ on PC12 cells. The $A\beta_{1-42}$ (2-16μM) significantly reduced PC12 cell viability with concentration-dependent when compared with the control group ($p<0.01$), which indicated that $A\beta_{1-42}$ could induce toxicity in PC12 cells (IC_{50} =16μM) (fig. 4A). Then, we determined whether SA had an adverse effect on cell viability. The result of the CCK-8 assay showed that different concentrations of SA (12.5-100μM) did not cause damage to cells.

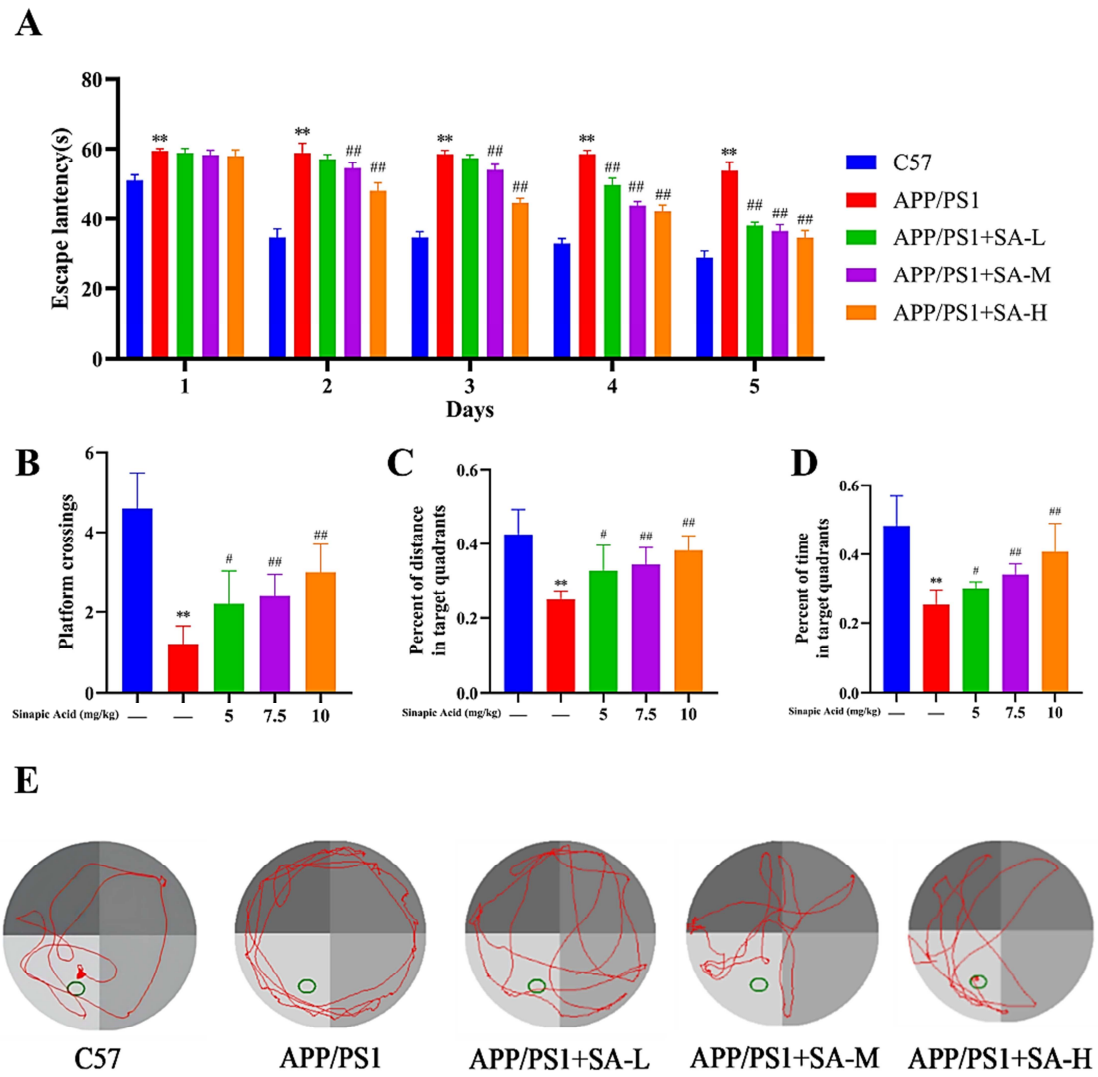

Fig. 1: Effects of SA on the mice's spatial learning and memory abilities in the MWM test. (A) Escape latencies in each group's visible and hidden platforms during MWM task training. (B)Number of crossing platforms. (C)Percent of distance in the target quadrant. (D) Percent of time in the target quadrant. (E)Swimming trajectory diagrams of mice during space exploration. The data are presented as the mean ± SEM, n = 5; *p<0.05, **p<0.01 vs. the WT group, $^{\#}$p< 0.05, $^{\#\#}$p<0.01 vs. the APP/PS1 group and each experiment was repeated three times.

The concentration of SA that reduces cell viability is 200μM (p<0.05) (fig. 4B). Next, we selected 2μM $A\beta_{1-42}$ and 25, 50 and 100μM SA in the following experiment. The result of the CCK-8 assay revealed that the cell viability after treatment with 2μM $A\beta_{1-42}$ was 81.97% (p<0.01), while the SA treatment was 87.00%, 89.08%, and 92.11%, respectively (the control group was 100%) (fig. 4C).

Effect of SA on Aβ1–42-Induced Microscopic Morphology in PC12 Cell Injury

According to fig. 5A, exposure of PC12 cells to 2μM $A\beta_{1-42}$ showed nuclear condensation, bright blue nuclei, or even fragmented nuclei, a classic feature of apoptosis compared with the control group. The number of apoptotic bodies decreased, accompanied by a corresponding reduction in nuclear-condensed cells when PC12 cells were treated with 25, 50 and 100mM SA. Besides, to determine whether SA could restrain apoptosis induced by $A\beta_{1-42}$, apoptosis of cells was examined by Calcein/PI staining. The living cells had been stained green, whereas the dead cells had appeared red. As shown in fig. 5B-D, after treatment with $A\beta_{1-42}$, the red increased and green fluorescence decreased. After SA treatment, fluorescence shifts from red to green as the concentration increases. The results confirmed that apoptosis was induced by $A\beta_{1-42}$; however, SA could inhibit this process.

Effects of SA on Aβ1–42-induced Apoptosis in PC12 Cell Injury

In fig. 6A, $A\beta_{1-42}$ is revealed to promote cell apoptosis (p<0.01). Nevertheless, incubation with SA could decrease apoptosis significantly at all concentrations (p< 0.05 or p<0.01). Compared with the control group,

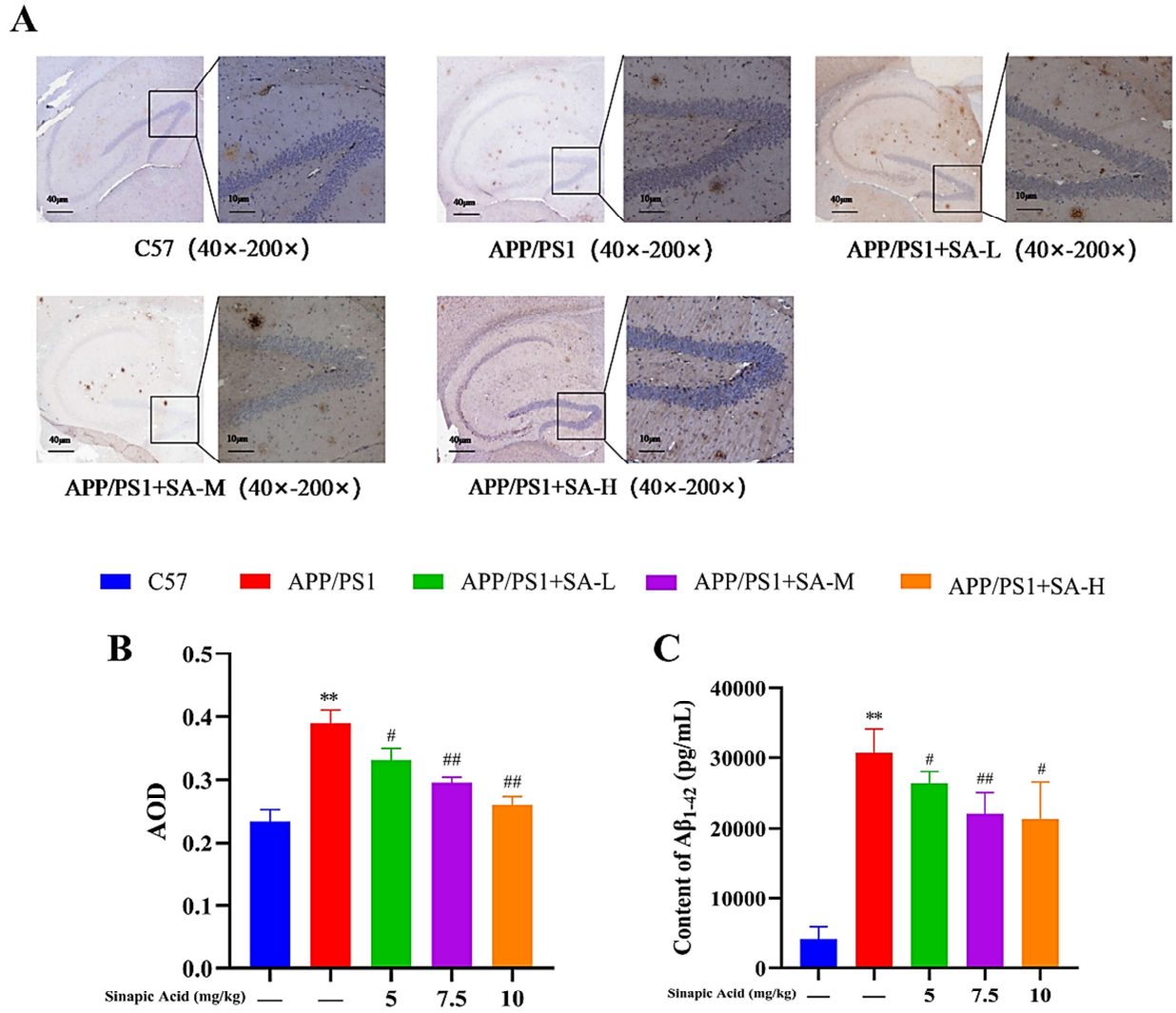

Fig. 2: Effects of SA on the plaque of Aβ in the hippocampus tissue of the mice. (A) Images of immunofluorescent co-staining. (B)The average optical density value (AOD). (C)The content of $A\beta_{1-42}$ in the hippocampus tissue of the mice. The data are presented as the mean ± SEM, n = 5; **p<0.01 vs. the WT group, #p<0.05, ##p<0.01 vs. the APP/PS1 group and each experiment was repeated three times.

treatment with $A\beta_{1-42}$ significantly reduced the Bcl-2/Bax ratio and increased caspase-3 levels (p<0.01). However, SA upregulated the ratio of Bcl-2/Bax and decreased the protein expression of Caspase-3 significantly (p<0.05 or p<0.01) (fig. 6B). Overall, SA could suppress neuronal death.

Effects of SA on Aβ1–42-induced the Protein Expression of P13K/Akt/GSK3β in PC12 Cell Injury

As shown in fig. 7, we pretreated PC12 cells with 10μM LY294002 for 0.5h; the expression of P13K, Akt and GSK3β in each group was similar; however, $A\beta_{1-42}$ decreased the expression level of p-P13K, p-Akt and p-GSK3β, p-P13K/t-P13K, p-Akt/t-Akt and GSK3β/p-GSK3β were decreased correspondingly (p<0.01). SA treatment resulted in higher p-p13k/t-P13K and p-akt/t-Akt ratios than the $A\beta_{1-42}$ treatment group (p<0.05 or p<0.01). Compared to $A\beta_{1-42}$ and SA treated group, the ratio of p-PI3K/PI3K, p-Akt/Akt and GSK3β/p-GSK3β markedly eliminated by the pre-incubated with inhibitor LY294002 (p<0.01).

The above data confirmed that SA had the function of protecting PC12 cells from $A\beta_{1-42}$ induced damage, as it could regulate the PI3K/Akt/GSK3β signaling pathway.

DISCUSSION

Recent investigations considered abnormal Aβ deposition one of AD's primary pathogenesis (Greenberg *et al.*, 2020). Aβ includes different Aβ fragments, especially the $A\beta_{1-42}$ peptide, which has more neurotoxicity and could cause neuron loss (Jonson *et al.*, 2018). Therefore, inhibiting cell apoptosis induced by Aβ is an effective

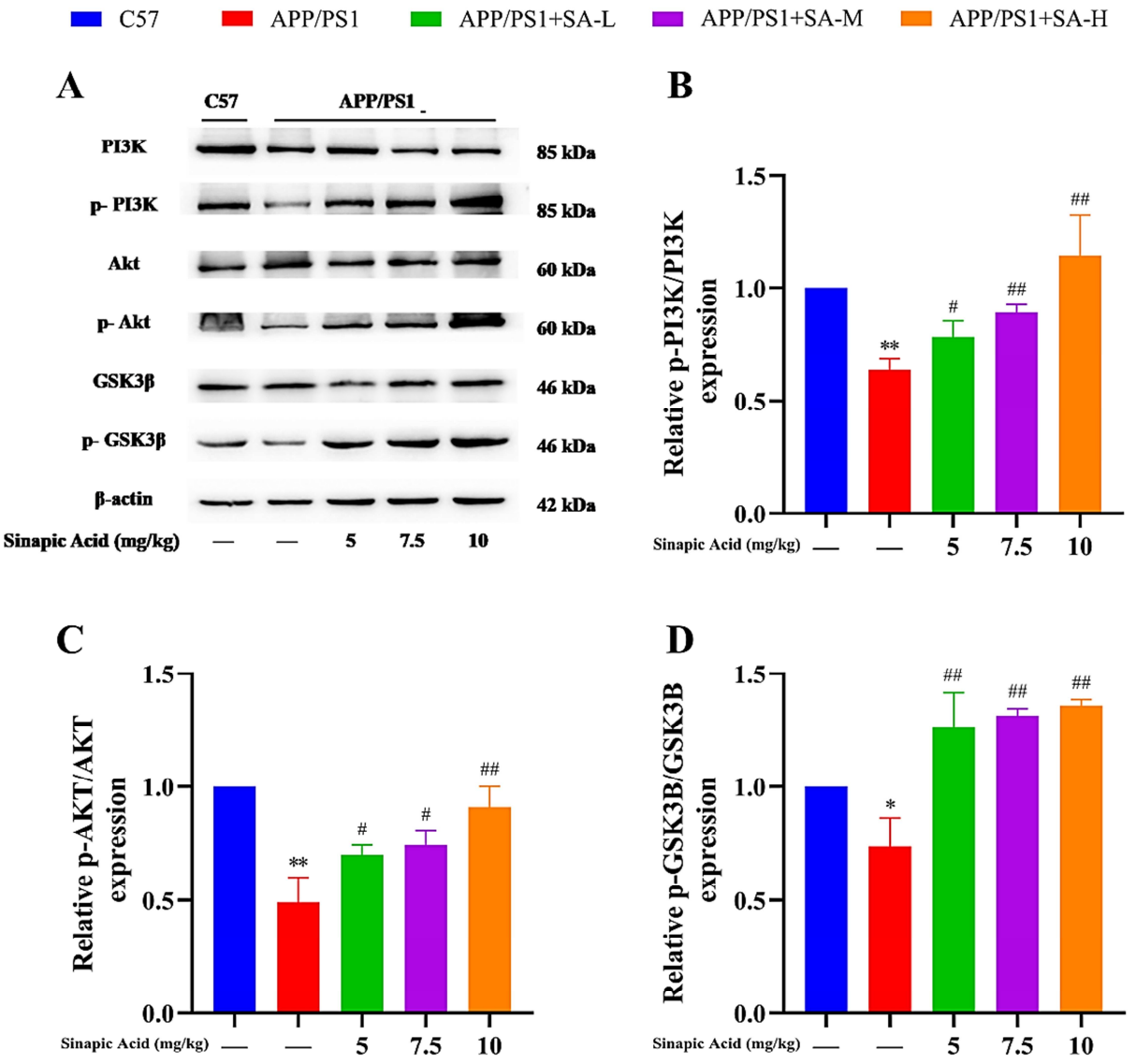

Fig. 3: Effect of SA on the protein expression of P13K/Akt/GSK3β in hippocampus tissue in mice. (A) Western blotting in each group. (B, C, D) The protein expression levels of P13K, p-P13K, Akt, p-Akt, GSK3β and p-GSK3β were determined by Western blot. Quantitative protein levels were normalized with β-actin. The data are presented as the mean ± SEM, n = 3; **p<0.01 vs. the control group, #p<0.05, ##p<0.01 vs. the $A\beta_{1-42}$ group, and each experiment was repeated three times.

method for treating AD. Consequently, it is currently considered that inhibiting the cell apoptosis induced by Aβ and reducing Aβ neurotoxicity is an effective therapy in treating AD. Pharmacological studies have found that SA could improve $A\beta_{1-42}$-induced cognitive impairment and reduce damage to hippocampal neurons as a neuroprotective agent through exhibiting neuroprotective effects; furthermore, SA could ameliorate the cognitive impairments arising from hypoxia and scopolamine exposure in Alzheimer's disease model, while simultaneously suppressing the memory deficits triggered by potassium cyanide (KCN) (Farzan *et al*., 2024; Lee *et al*., 2023; Xu *et al*., 2021). As expected, our findings implied SA could ameliorate cognitive impairment by improving long-term learning and memory.

The hippocampus is a key structure for learning and memory in the brain, with a large number of neurons. In the early stages of AD, the hippocampus is the most susceptible area to damage and a marker of pathological changes (Wang *et al*., 2021). Abnormal deposition of Aβ in the brain is a key cause of AD, which in turn induces NFT formation, inflammatory response, oxidative stress, neuronal loss and vascular damage (Jucker *et al*., 2023). Therefore, reducing the abnormal deposition of Aβ in the hippocampus as the site is crucial. In our study, deposition

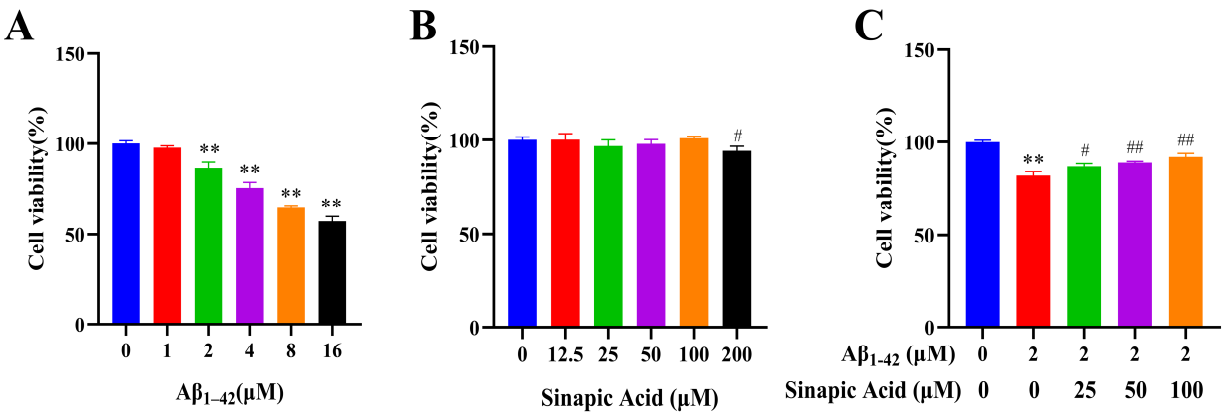

Fig. 4: Effect of different concentrations of $A\beta_{1-42}$ or SA of PC12 cell viability. (A)Cell viability of different doses of $A\beta_{1-42}$ (0, 1, 2, 4, 8, 16μM) for 24h. (B)Cell viability of different doses of SA (0, 12.5, 25, 50, 100, 200mM) for 24h. (C) Cell viability of 2μM $A\beta_{1-42}$ for 24h and different concentrations of SA (25, 50, 100μM) for another 24h. The data are presented as the mean ± SEM, n=3; **p<0.01 vs. the control group, $^{\#}$p<0.05, $^{\#\#}$p<0.01vs. The $A\beta_{1-42}$ group and each experiment was repeated three times.

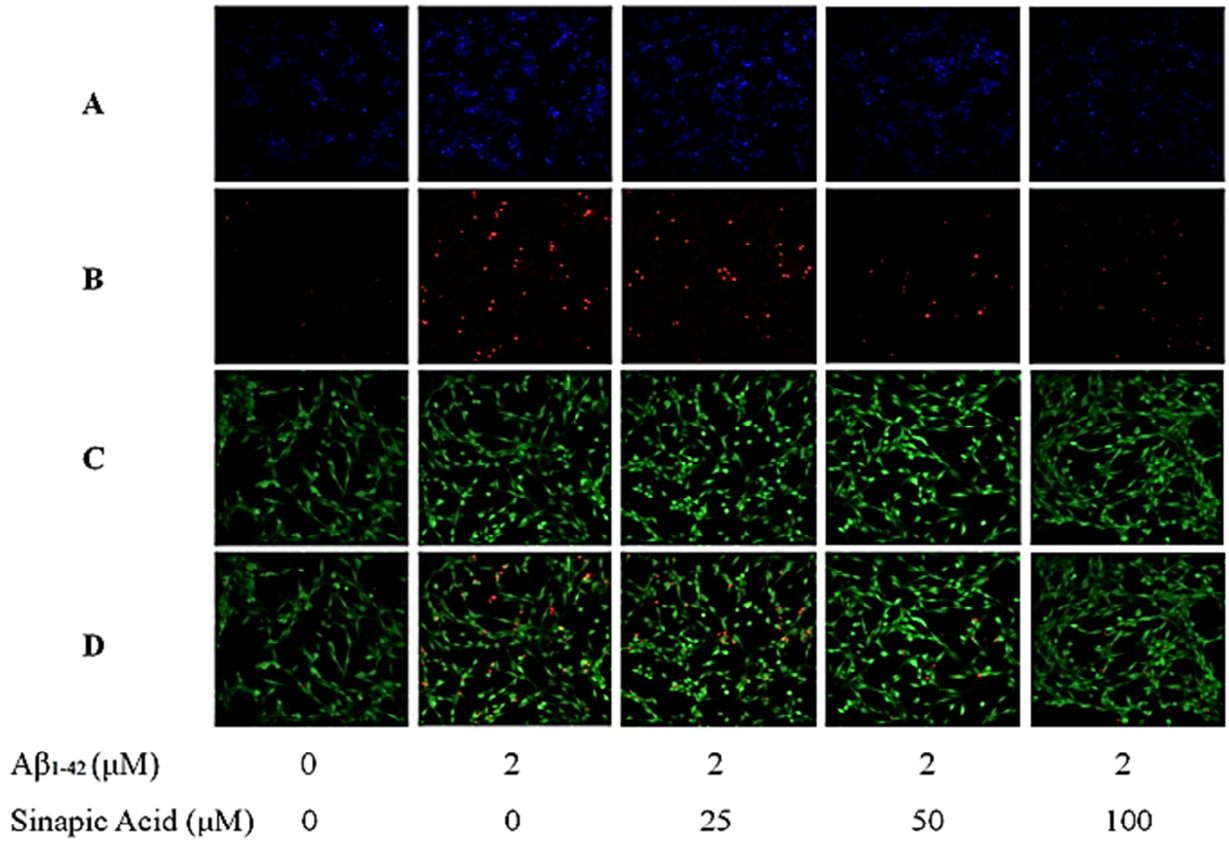

Fig. 5: Effects of SA on $A\beta_{1-42}$-Induced morphological change of PC12 cells. (A) Hoechst 33342 staining (100×). (B) PI staining (100 ×). (C) Calcein AM staining (100 ×). (D) B and C merge. Each experiment was repeated three times.

of Aβ declined in the hippocampus of APP/PS1 mice after the administration of SA. This is consistent with the results of ELISA and immunohistochemistry.

Similarly, *in vitro* studies have found the neuroprotective function of SA and its derivatives (Farzan *et al*., 2024). Due to neurons' similar physiological and morphological characteristics, the PC12 cell line has been used as an *in vitro* model for neurodegenerative diseases, including AD (Zhang *et al*., 2024). Therefore, our study used $A\beta_{1-42}$-induced PC12 cells as an AD neurotoxicity model *in vitro*. Firstly, $A\beta_{1-42}$ had a certain appearance of cytotoxicity by decreasing the cellular survival rate. Moreover, the findings revealed that SA exhibited the ability to safeguard PC12 cells from neurotoxicity triggered by $A\beta_{1-42}$.

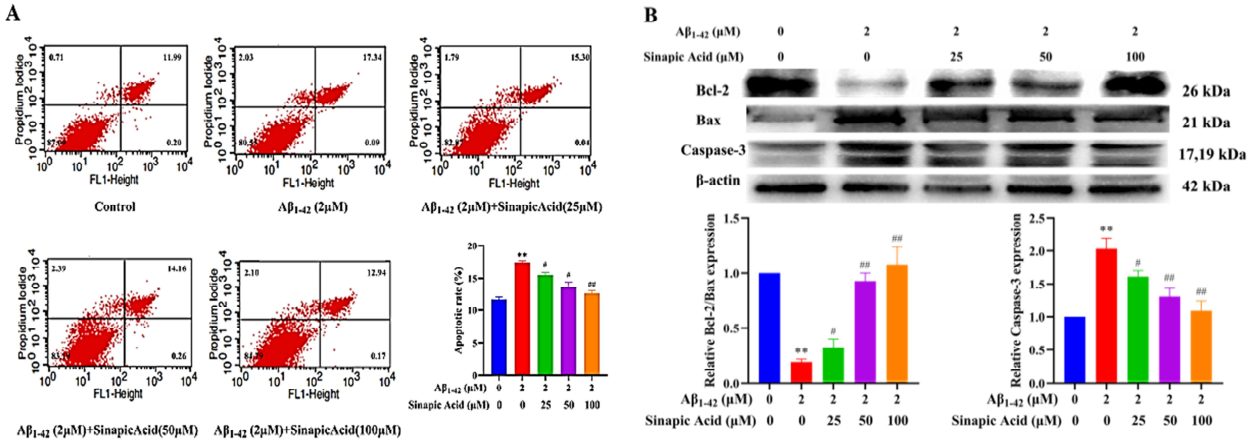

Fig. 6: Effect of SA on Aβ$_{1-42}$-induced apoptosis of PC12 cells. (A) Apoptotic cell death was analyzed by flow cytometry. The number of counts in the up-right (UR) and down-right (DR) regions of the flow cytometry quadrant were counted as apoptotic cells. (B) Expression levels and quantification of Bcl-2/Bax ratio and Caspase-3 were determined by Western blot. Quantitative protein levels were normalized with β-actin. The data are presented as the mean ± SEM, n = 3; **p<0.01 vs. the control group, $^{\#}$p<0.05,$^{\#\#}$p<0.01 vs. the Aβ$_{1-42}$ group and each experiment was repeated three times.

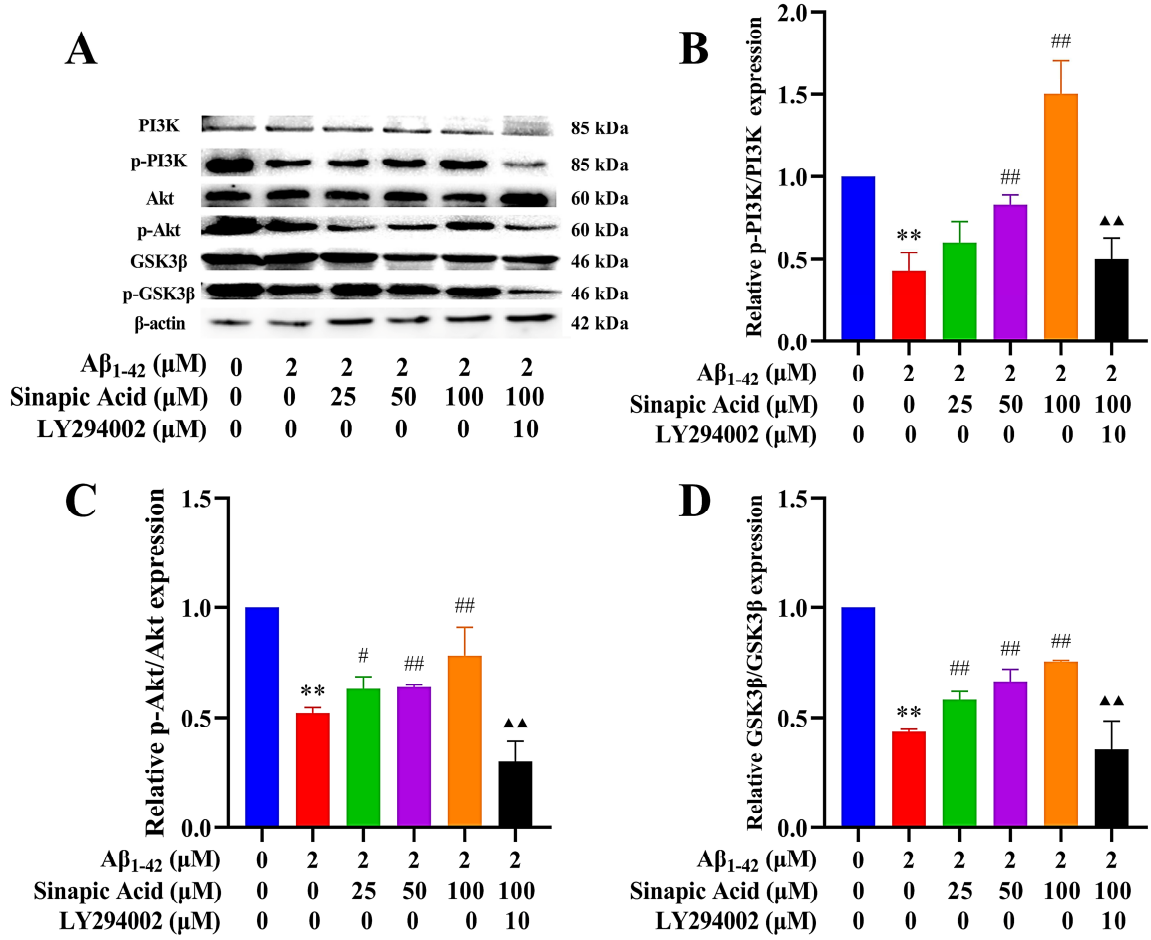

Fig. 7: Effect of SA on Aβ$_{1-42}$-induced P13K/Akt/GSK3β protein expression of PC12 cells. (A) Western blotting in each group. (B, C, D) The protein expression levels of P13K, p-P13K, Akt, p-Akt, GSK3β, and p-GSK3β were determined by Western blot. Quantitative protein levels were normalized with β-actin. The data are presented as the mean ± SEM, n = 3; **p<0.01 vs. the control group, $^{\#}$p<0.05 and $^{\#\#}$p<0.01 vs. the Aβ$_{1-42}$ group, $^{\blacktriangle\blacktriangle}$p<0.01 vs. the SA (100μM) group and each experiment was repeated three times.

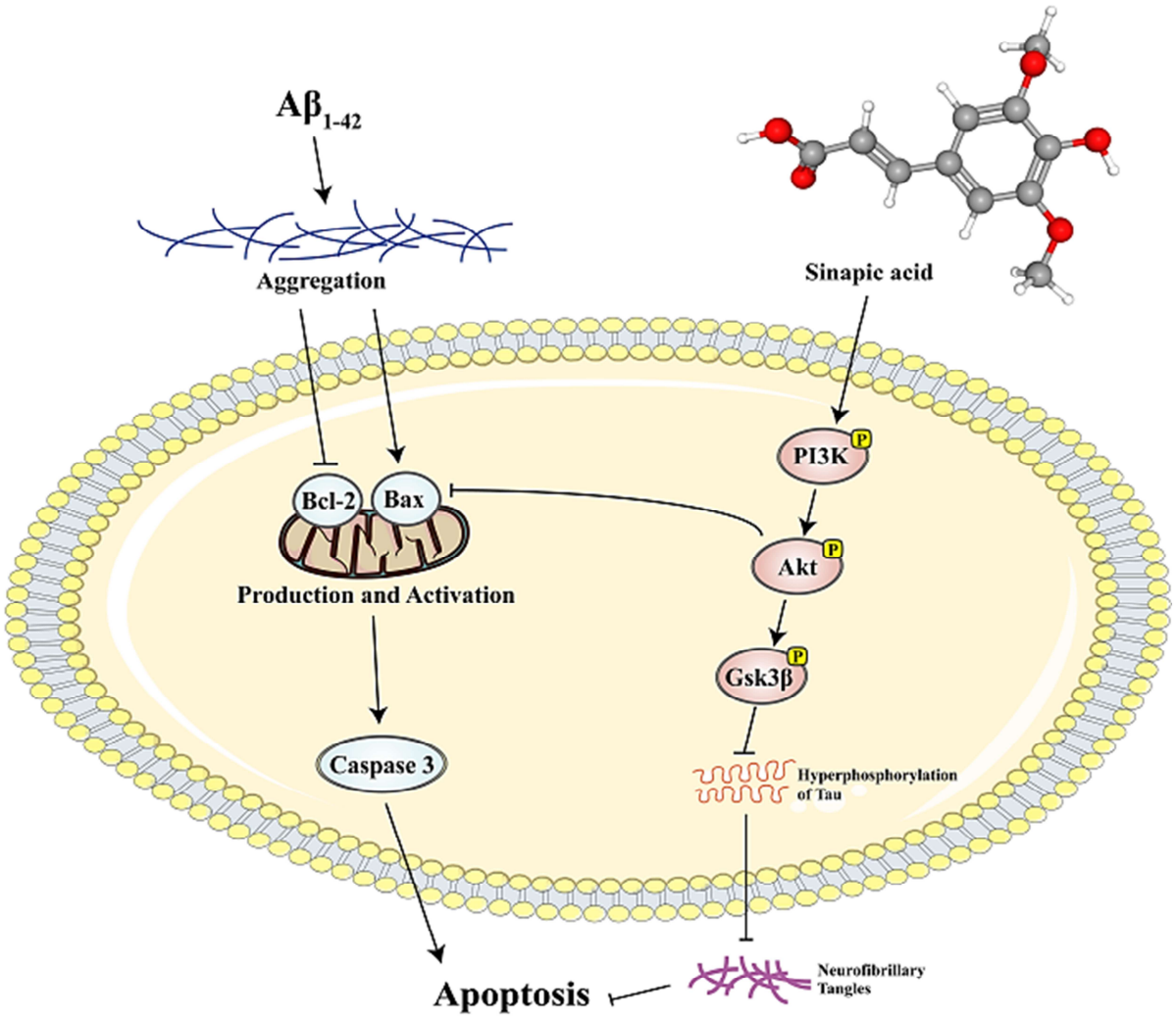

Fig. 8: Schematic diagram of the possible mechanism underlying the neuroprotection of SA on PC12 cells.

Apoptosis is a special way of cell death different from cytonecrosis, which follows its programmed cell death under gene regulation and shows unique morphological characteristics, such as shrinkage of cell volume, concentration of cytoplasm, pyknosis of nucleus, nucleolysis and apoptotic bodies (Newton *et al*., 2024). Bcl-2 is the primary gene that inhibits apoptosis. On the contrary, the Bax protein promotes apoptosis. Survival proteins and apoptosis proteins can form dimers, and their relative balance is the key to determining the survival of cells (Suraweera *et al*., 2022). Despite this, the disparity in levels between survival proteins and apoptosis proteins triggers the liberation of cytochrome C, ultimately resulting in the activation of caspases and the induction of apoptosis (Santucci *et al*., 2019). Apoptosis of nerve cells may be one of the key factors inducing AD (Tungalag and Yang, 2021). Consistent with relevant research, $A\beta_{1-42}$ induced apoptosis in PC12 cells by increasing Bax and caspase-3 and decreased Bcl-2 expression. Moreover, SA could significantly inhibit the reduction of Bcl-2 and the elevation of Bax and caspase-3. Therefore, it can be inferred that SA is provided with neuroprotective effects by inhibiting apoptosis.

PI3K is one of the important kinases of signal transduction in cells, which is composed of two binding sites of regulatory subunit p85 and catalytic subunit p110. When acted by extra cellular stimulation signal molecules, p85 phosphorylates and releases the inhibition of p110, activating the PI3K pathway (Ren *et al*., 2019; Zhi *et al*., 2023). Akt is a prosurvival kinase that acts as a direct downstream target of PI3K and is activated by the phosphorylation at the Ser473, which plays an important role in the PI3K signal transduction pathway. PI3K increases neuroprotective effects by regulating phosphorylation levels and activating Akt (Zhang *et al*., 2018). Activated Akt can phosphorylate GSK3, mainly by initiating downstream cascade reactions of PI3K/Akt. In recent research, GSK3β Hyperactivating can directly induce neuronal cell death and abnormal tau protein hyperphosphorylation, which can cause the occurrence of AD. However, the upregulation of GSK3β

phosphorylation level may inhibit GSK3β and improve the damage of nerve cells (Lauretti *et al*., 2020). Other studies showed that SA promoted the browning of 3T3-L1 adipocytes via the p38 MAPK/CREB pathway, which is downstream of the PI3K/Akt/GSK3β pathway, suggesting that SA may participate in the regulation of PI3K/Akt/GSK3β signal pathway (Lauretti *et al*., 2020). *In vivo* studies showed that the SA could activate the phosphorylation of PI3K, Akt and GSK3 β in hippocampal neurons of AD mice. Meanwhile, the results *in vitro* showed that Aβ treatment significantly decreased the ratio of p-PI3K/PI3K, p-Akt/Akt, and p-GSK3β/GSK3β, while SA upregulated the levels of PI3K/Akt/GSK3β phosphorylation noticeably. However, LY294002, a PI3K inhibitor, abated p-PI3K, p-Akt and p-GSK3β expression. These findings suggested that SA exhibited a neuroprotective effect against $A\beta_{1-42}$-induced apoptosis of neurons through activation of the P13K/Akt/GSK3β signaling pathway in APP/PS1 mouse model and PC12 cells of AD.

CONCLUSION

In summary, the current study was the first to note that SA could improve cognitive impairment, reduce the content of $A\beta_{1-42}$ to reduce Aβ deposition and amyloid plaques in the hippocampus of APP/PS1 mice, protect PC12 cells against $A\beta_{1-42}$-induced neurotoxicity as a neuroprotective agent as well through activating of PI3K/Akt/GSK3β pathway. Therefore, SA might be a potential candidate for treating AD. We will further conduct *in vitro* studies or other models *in vivo* to understand more in-depth molecular mechanisms of SA. A possible molecular mechanism of neuroprotective effects of SA has been described in fig. 8.

ACKNOWLEDGEMENT

This study was financially supported by Fund project of Qiqihar Academy of Medical Sciences (Grant No. QMSI 2024M-12, QMSI2019L-05), Research Project on Traditional Chinese Medicine of Heilongjiang Province (ZHY2024-279), Scientific Research Topics of Heilongjiang Provincial Health and Wellness Commission (No.20240202040348).

REFERENCES

Breijyeh Z and Karaman R (2020). Comprehensive review on Alzheimer's disease: Causes and treatment (2020). *Molecules,* **25**(24): 5789.

Caruso G, Spampinato SF, Cardaci V, Caraci F, Sortino MA and Merlo S (2019). β-amyloid and oxidative stress: Perspectives in drug development. *Curr Pharm Des.,* **25**(45): 4771-4781.

Farzan M, Abedi B, Bhia I, Madanipour A, Farzan M, Bhia M, Aghaei A, Kheirollahi I, Motallebi M, Amini-Khoei H and Ertas YN (2024). Pharmacological Activities and molecular mechanisms of sinapic acid in neurological disorders. *ACS Chem Neurosci.*, **15**(16): 2966-2981.

Greenberg SM, Bacskai BJ, Hernandez-Guillamon M, Pruzin J, Sperling R and Van Veluw SJ (2020). Cerebral amyloid angiopathy and Alzheimer disease - one peptide, two pathways. *Nat Rev Neurol.,* **16**(1): 30-42.

Ikeda Y, Nagase N, Tsuji A, Kitagishi Y and Matsuda S (2021). Neuroprotection by dipeptidyl-peptidase-4 inhibitors and glucagon-like peptide-1 analogs via the modulation of AKT-signaling pathway in Alzheimer's disease. *World J Biol Chem*., **12**(6):104-113.

Jonson M, Nystrom S, Sandberg A, Carlback M, Michno W, Hanrieder J, Starkenberg A, Nilsson KPR, Thor S, Hammarstrom P (2018). Aggregated Aβ1-42 is selectively toxic for neurons, whereas glial cells produce mature fibrils with low toxicity in drosophila. *Cell Chem. Biol.,* **25**(5): 595-610.e5.

Jucker M and Walker LC (2023). Alzheimer's disease: From immunotherapy to immunoprevention. *Cell*, **186**(20): 4260-4270.

Kumar M and Bansal N (2022). Implications of Phosphoinositide 3-Kinase-Akt (PI3K-Akt) pathway in the pathogenesis of Alzheimer's disease. *Mol. Neurobiol*., **59**(1): 354-385.

Lauretti E, Dincer O and Pratico D (2020). Glycogen synthase kinase-3 signaling in Alzheimer's disease. *Biochim Biophys Acta Mol Cell Res.,* **1867**(5): 118664.

Lee IS, Choi GY, Sreelatha I, Yoon JW, Youn SH, Maeng S and Park JH (2023). Effect of sinapic acid on scopolamine-induced learning and memory impairment in SD rats. *Brain Sci.,* **13**(3): 427.

Li X, Sun Y, Zhou Z, Li J, Liu S, Chen L, Shi Y, Wang M, Zhu Z, Wang G and Lu Q (2024). Deep learning-driven exploration of pyrroloquinoline quinone neuroprotective activity in Alzheimer's disease. *Adv. Sci. (Weinh)*, **11**(18): e2308970.

Liu QQ, Ding SK, Zhang H and Shang YZ (2022). The Molecular mechanism of *Scutellaria baicalensis* Georgi stems and leaves flavonoids in promoting neurogenesis and improving memory impairment by the PI3K-AKT-CREB signaling pathway in rats. *Comb. Chem. High Throughput Screen,* **25**(5): 919-933.

Matsuda S, Ikeda Y, Murakami M, Nakagawa Y, Tsuji A and Kitagishi Y (2019). Roles of PI3K/AKT/GSK3 pathway involved in psychiatric illnesses. *Diseases,* **7**(1): 22.

Newton K, Strasser A, Kayagaki N and Dixit VM (2024). Cell death. *Cell*, **187**(2): 235-256.

Pandi A and Kalappan VM (2021). Pharmacological and therapeutic applications of sinapic acid-an updated review. *Mol. Biol. Rep.,* **48**(4): 3733-3745.

Rajendran K and Krishnan UM (2024). Biomarkers in Alzheimer's disease. *Clin. Chim. Acta.,* **562**: 119857.

Ren L, Zhou X, Huang X, Wang C and Li Y (2019). The IRS/PI3K/Akt signaling pathway mediates olanzapine-induced hepatic insulin resistance in male rats. *Life Sci.,* **217**: 229-236.

Santucci R, Sinibaldi F, Cozza P, Polticelli F and Fiorucci L (2019). Cytochrome C: An extreme multifunctional protein with a key role in cell fate. *Int J Biol Macromol.,* **136**: 1237-1246.

Suraweera CD, Banjara S, Hinds MG and Kvansakul M (2022). Metazoans and intrinsic apoptosis: An evolutionary analysis of the Bcl-2 family. *Int. J. Mol. Sci.,* **23**(7): 3691.

Tungalag T and Yang DK (2021). Sinapic Acid Protects SH-SY5Y Human neuroblastoma cells against 6-hydroxydopamine-induced neurotoxicity. *Bio-medicines,* **9**(3): 295.

Wang J, Liu B, Xu Y, Yang M, Wang C, Song M, Liu J, Wang W, You J, Sun F, Wang D, Liu D and Yan H (2021). Activation of CREB-mediated autophagy by thioperamide ameliorates β-amyloid pathology and cognition in Alzheimer's disease. *Aging Cell.,* **20**(3): e13333.

Wang Y, Hu H, Liu X and Guo X (2023). Hypoglycemic medicines in the treatment of Alzheimer's disease: Pathophysiological links between AD and glucose metabolism. *Front Pharmacol.*, **14**: 1138499.

Xu H, Zhou Q, Liu B, Cheng KW, Chen F and Wang M (2021). Neuroprotective potential of mung bean (*Vigna radiata* L.) polyphenols in Alzheimer's disease: A review. *J. Agric. Food Chem*., **69**(39): 11554-11571.

Zhang S, Xue R, Geng Y, Wang H and Li W (2020). Fisetin prevents HT22 cells from high glucose-induced neurotoxicity via PI3K/Akt/CREB signaling pathway. *Front. Neurosci*., **14**: 241.

Zhang W, Liu X and Li Q (2018). Protective effects of oleuropein against cerebral ischemia/reperfusion by inhibiting neuronal apoptosis. *Med. Sci. Monit.,* **24**: 6587-6598.

Zhang X, Bao M, Zhang J, Zhu L, Wang D, Liu X, Xu L, Luan L, Liu Y and Liu Y (2024). Neuroprotective mechanism of ribisin A on H_2O_2-induced PC12 cell injury model. *Tissue Cell*, **87**: 102322.

Zhi F, Li B, Zhang C, Xia F, Wang R, Xie W, Cai S, Zhang D, Kong R, Hu Y, Yang Y, Peng Y and Cui J (2023). NLRP6 potentiates PI3K/AKT signalling by promoting autophagic degradation of p85α to drive tumorigenesis. *Nat. Commun*., **14**(1): 6069.